Large-signal optically controlled HEMT model and oscillator design

G.Zhang
R.D.Pollard
C.M.Snowden

Indexing terms: HEMT oscillator, Optical tuning, Oscillator design, Signal classification

Abstract: A new large-signal equivalent circuit model of a pHEMT with and without illumination has been developed. A HEMT oscillator operating at approximately 31GHz has been designed and tested, based on this model. The optical tuning frequency range of 31MHz under a halogen lamp and 60MHz under a GaAs laser illumination has been observed.

1 Introduction

Direct optical control of microwave semiconductor devices has been applied to achieve various functions of microwave circuits including the gain control of amplifiers, oscillator tuning, injection-locking, frequency modulation, switching, mixing and phase shifting [1–3].

Several authors have investigated the DC and microwave characteristics of optically controlled HEMTs [2, 3]. Their studies suggest that the photo response is due to optically injected carriers, causing the photoconductive effect and a photogenerated gate current resulting in a voltage drop across the gate resistance, called the photovoltaic effect. Both effects on the small signal equivalent circuit model elements have heen investigated. Oscillator design based on this model has also been studied [4, 5]. However, there is a lack of a general large-signal model of optically controlled HEMTs, which might be used to predict accurately the characteristics of various functions of optically controlled microwave circuits under large signal conditions.

This paper develops a new large signal equivalent circuit model which accounts for the behaviour with and without illumination and its application to oscillator design. This study shows that the photoconductive effect dominates. A high performance GaAs chip pHEMT provided by Hewlett-Packard with 0.25μm gate length and 4 × 30μm gate width was measured with a HP8510C network analyser over the frequency range from 1 to 50GHz under multibias conditions, using a wafer probe with and without illumination. For convenience, a noncoherent optical source (a halogen lamp) was used for the device characterisation. The small-signal equivalent circuit elements were extracted employing the so-called 'hot-cold' modelling extraction technique [6]. The extrinsic element parameters were uniquely extracted by optimising the unbiased and pinch-off cold equivalent circuit model; and the intrinsic element parameters were then analytically derived from the S-parameters. A DC model proposed by Angelov [7] was then used to model the DC drain current characteristics. All the RF characteristics of the major nonlinear equivalent circuit elements, C_{gs}, C_{gd}, C_{ds} and g_m were also modelled [8]. Based on this model, an oscillator with series feedback, common source configuration was simulated and tested. Both the noncoherent source (a halogen lamp) and the coherent source (a GaAs laser with the wavelength of 0.83μm) were used. Optical tuning frequency ranges of 31MHz under lamp illumination and 60MHz under GaAs laser illumination were observed. Output power of 3.4dBm and 3dBm were obtained with and without the laser illumination.

Optically tuned HEMT oscillators are very attractive for application in microwave and millimetre-wave optical fibre communication and control systems, especially for phased array antennae.

2 Basic mechanism of HEMT operation under illumination

Fig. 1 shows the vertical structure of a pHEMT and its energy band diagram. When the device is illuminated

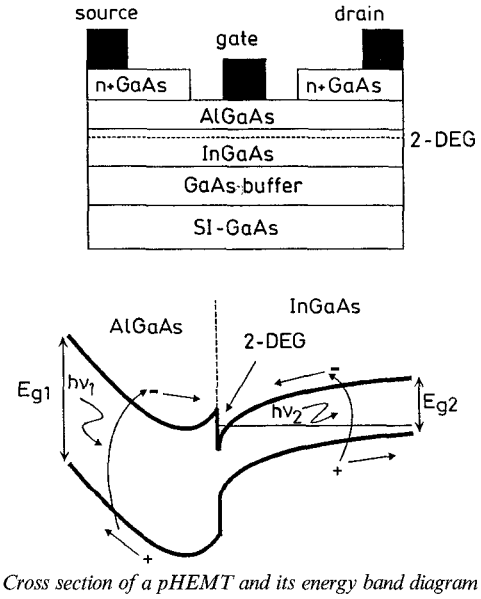

Fig. 1 *Cross section of a pHEMT and its energy band diagram*

IEE Proceedings online no. 19960750

Paper first received 4th April and in revised form 5th July 1996

The authors are with the Microwave and Terahertz Group, Department of Electronic and Electrical Engineering, University of Leeds, Leeds LS2 9JT, UK

by photons of energy equal to or greater than the semiconductor band gap, free electron-hole pairs will be generated in the active layers. The major photoeffects of pHEMTs caused by illumination are band-to-band photon absorption in the InGaAs and the AlGaAs layers. The electron-hole pairs are generated in these regions.

Photons absorbed in the InGaAs layer give rise to an increase in the electron concentration. The electric field associated with the heterojunction sweeps the photoelectrons into the 2-DEG channel, thereby increasing the drain current and the photoconductive effect occurs. If photons are also absorbed in the AlGaAs layer, the photogenerated electron-hole pairs will be separated by the built-in electric field which sweeps the electrons to the 2-DEG while the holes enhance the gate current. When a high gate bias resistance is present, the photovoltaic effect arises from the gate current flowing through the gate resistance.

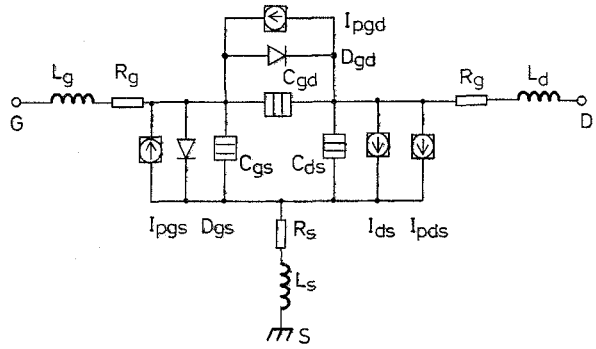

Fig. 2 *Large-signal equivalent circuit of a HEMT with illumination*

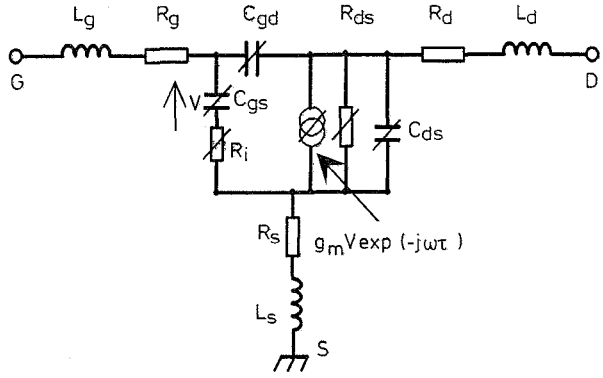

Fig. 3 *Small-signal equivalent circuit of a HEMT with marked elements changed by illumination*

3 Large-signal model of the pHEMT with and without illumination

A complete large signal model of a pHEMT device is shown in Fig. 2 where I_{pdg} and I_{pgs} are photocurrent sources leading to photovoltaic effect and I_{pds} is a photoconductive current source. It is necessary that all RF equivalent circuit elements be extracted from S-parameters at multiple bias points. The small signal equivalent circuit model of pHEMTs is shown in Fig. 3. The elements in this model can be classified in two categories: (i) the intrinsic elements g_m, g_{ds}, C_{gs}, C_{gd}, C_{ds}, R_i and τ, which are dependent on the bias conditions; (ii) the extrinsic elements L_g, R_g, I_{pdg}, R_s, L_d and R_d, which are independent of the bias conditions. For a MESFET, its extrinsic elements are usually extracted by 'cold' measurement with large positive and well below pinch-off V_{GS} and with $V_{DS} = 0$ [6]. However, positive V_{GS} bias should be avoided to extract the elements of a HEMT, since this causes a parasitic MESFET effect inside the HEMT which leads to an inaccuracy for the extrinsic resistance [9]. In this paper, models for the 'cold' device with bias values of zero and well below pinch-off were used to extract all the extrinsic elements; the intrinsic element parameters were subsequently derived analytically.

The large signal model is then developed based on the DC characteristics and the small signal equivalent circuit elements at multiple biases. The Angelov model [7] is used for the $I_{DS}[V_{GS}, V_{DS}]$ DC characteristics as follows:

$$I_{DS} = A(1+\tanh(k_1V+k_2V^2+k_3V^3))(1+k_4V_{DS})\tanh(k_5V_{DS}) \quad (1)$$

All the RF characteristics of the major nonlinear equivalent circuit elements, C_{gs}, C_{gd}, C_{ds} and g_m are modelled as

$$C_{gs,gd,ds} = \frac{A(e^{(k_1V_{GS}+k_2V_{GS}^2+k_3V_{GS}^3)}+k_4(V_{GS}+V_{DS})10^{k_5(V_{GS}+V_{DS})})}{1+(k_6V_{GS}+k_7V_{GS}^2+k_8V_{GS}^3)10^{k_5V_{GS}}} \quad (2)$$

$$g_m = A(1-(\tanh(k_1V+k_2V^2+k_3V^3+k_4V^4))^2)(1+k_5V_{DS}+k_6V_{DS}^2)(k_1+2k_2V+3k_3V^2+4k_4V^3) \quad (3)$$

where

$$V = V_{GS} - k_7 - k_8V_{DS}$$

The extracted values of the coefficients of I_{DS}, C_{GS}, C_{GD}, C_{DS} and g_m are listed in Table 1. The calculated value of I_{DS} is presented in Fig. 4 compared with the extracted one. All the fitted and extracted results for I_{DS}, C_{GS}, C_{GD}, C_{DS} and g_m are shown in Figs. 5–8.

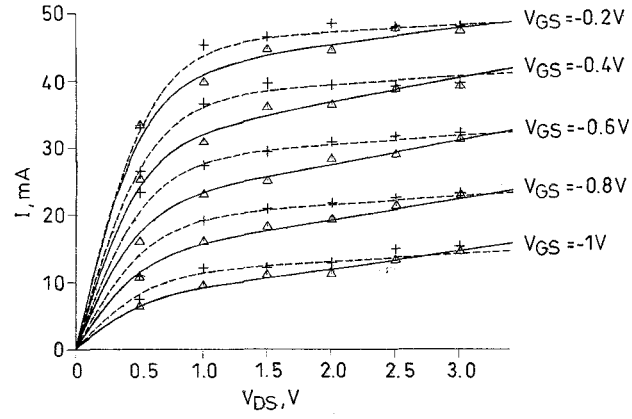

Fig. 4 *Measured and fitted DC I-V characteristics of the pHEMT with and without illumination*
——— fitted without illumination
- - - - fitted with illumination
△ extracted without illumination
\+ extracted with illumination

4 Oscillator simulation using one-port network theory

A simple series feedback common source configuration was chosen for the HEMT oscillator simulation, as shown in Fig. 9. The steady state conditions were satisfied during the oscillator simulation,

$$\mathrm{Im}(Y_D + Y_L) = 0 \quad (4)$$

and

$$\mathrm{Re}(Y_D + Y_L) = 0 \quad (5)$$

Table 1: Fitted coefficients of I_{DS}, C_{GS}, C_{GD}, C_{DS} and g_m

		A	k_1	k_2	k_3	k_4	k_5	k_6	k_7	k_8
I_{DS}, mA	dark	26.02	1.70	0.57	1.40	–	2.05	–	–0.48	–0.08
	light	28.30	1.60	0.02	0.90	–	1.80	–	–0.59	–0.03
C_{GS}, fF	dark	114.8	0.20	–	–	0.02	0.04	1.15	–0.10	–0.49
	light	105.3	0.06	–	–	0.10	–0.09	–0.75	–2.20	–1.20
C_{GD}, fF	dark	35.73	1.50	–	–	–0.56	–0.15	–1.64	3.19	0.93
	light	37.82	1.60	–	–	–0.75	–0.17	–3.05	1.99	1.00
C_{DS}, fF	dark	36.06	0.13	10.0	–1.32	–3.85	–0.97	0.33	0.78	0.22
	light	35.15	0.06	9.87	–1.36	–1.34	3.74	0.18	4.42	0.11
g_m, S	dark	0.040	1.20	–0.14	–0.23	–0.10	–0.08	–0.02	–0.54	–
	light	0.044	1.20	–0.10	0.28	–	–0.04	–	–0.53	–0.02

The simulation used the nearly sinusoidal approximation [10]. All of the design work was carried out with a commercially available simulator (HP-EEsof/Microwave Design System) using a symbolically-defined model for the pHEMT with parameters from eqns. 1–3 and Table 1.

5 Experimental results and discussion

The experiments were carried out using a high performance chip pHEMT (with 0.25μm gate length and width 4 × 30μm gate), a noncoherent optical source (a halogen lamp) and a coherent optical source (a GaAs laser with a wavelength of 0.83μm, and output power of 1mW). Only the halogen lamp was used to characterise the device.

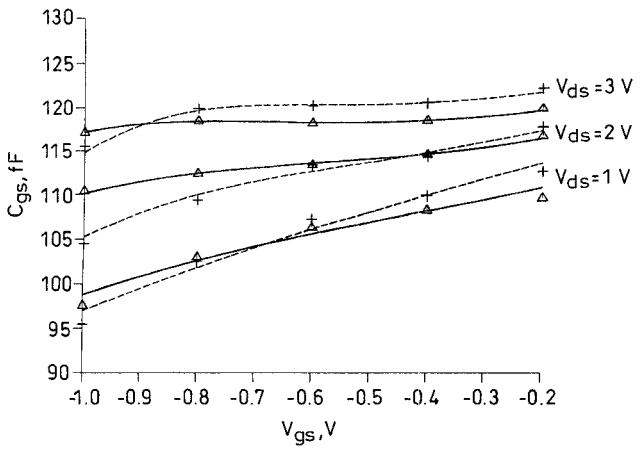

Fig. 5 *Bias dependence of C_{gs} with and without illumination*
——— fitted without illumination
– – – – fitted with illumination
△ extracted without illumination
\+ extracted with illumination

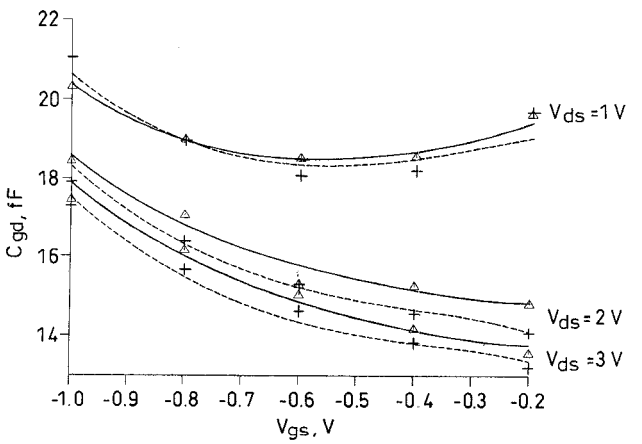

Fig. 6 *Bias dependence of C_{gd} with and without illumination*
——— fitted without illumination
– – – – fitted with illumination
△ extracted without illumination
\+ extracted with illumination

5.1 DC characteristics

The DC characteristics of the device were measured with the HP4145D parameter analyser. The measured drain-to-source current, I_{DS}, as a function of the drain-to-source voltage, V_{DS}, with and without illumination for the device is illustrated in Fig. 4. From the Figure, it is shown that, while there is a kink effect in the drain current without illumination [11], this effect vanishes under illumination due to the generated photocurrent being amplified by the traps in the buffer layer of the devices. These traps can be affected by V_{DS} [12] and therefore, the photoresponse of the DC drain current characteristics is dependent on V_{DS}.

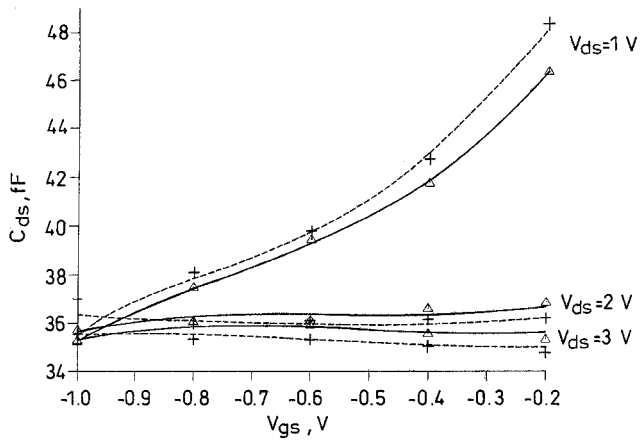

Fig. 7 *Bias dependence of C_{ds} with and without illumination*
——— fitted without illumination
– – – – fitted with illumination
△ extracted without illumination
\+ extracted with illumination

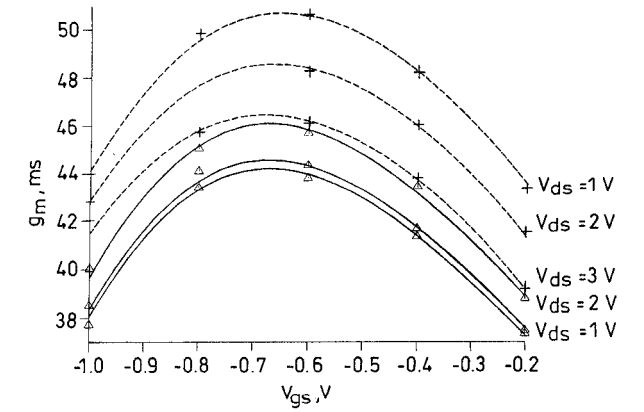

Fig. 8 *Bias dependence of g_m with and without illumination*
——— fitted without illumination
– – – – fitted with illumination
△ extracted without illumination
\+ extracted with illumination

5.2 Scattering parameters measurement

On-wafer multiple bias S-parameter measurement of the device was carried out with the HP8510C network analyser. Fig. 10 shows the S-parameters at a normal bias point (V_{GS} = –1, V_{DS} = 2) over the frequency range from 1 to 50GHz. It is observed that optical illumination has a little effect on s_{11}, s_{22} and s_{12}. However, s_{21} is significantly changed by the illumination.

5.3 Oscillator test

A HEMT oscillator operating at 31GHz has been realised in hybrid form. It was constructed on 10mil RT/Duroid 5880 substrate, using the Hewlett-Packard chip pHEMT which had been characterised previously. The layout of the oscillator is shown in Fig. 11. Both the halogen lamp and the GaAs laser have been used to test the HEMT oscillator. At a bias point of V_{GS} = –1V and V_{DS} = 2V, an optical tuning range of 31MHz and 60MHz has been observed from the oscillator under the lamp and the laser illumination, respectively. Output power was 3.4dBm and 3dBm with and without laser illumination.

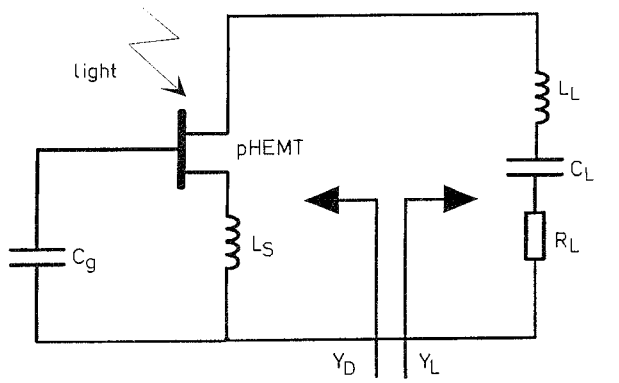

Fig. 9 *Schematic of the series feedback common source HEMT oscillator*
——— without illumination
– – – – with illumination
a S_{11} *b* S_{12}
c S_{21} *d* S_{22}

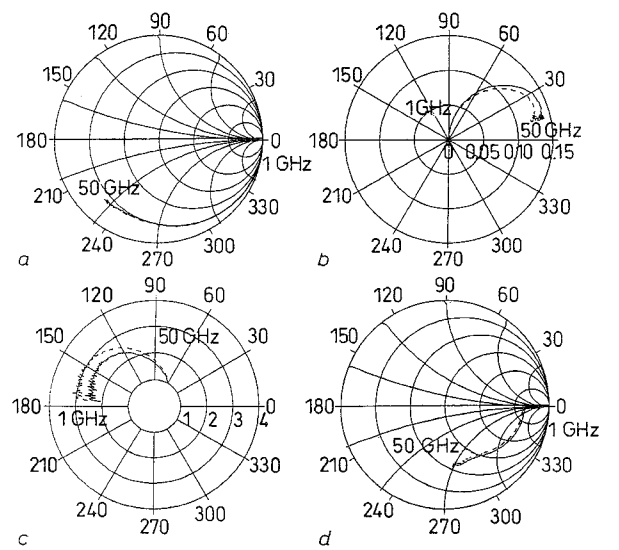

Fig. 10 *Measured S-parameters of the pHEMT with and without illumination*

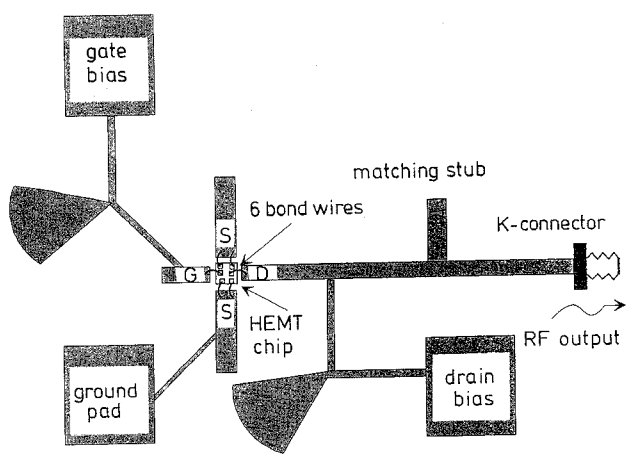

Fig. 11 *Layout of a microstrip HEMT oscillator operating around 31 GHz*

6 Conclusions

A new large signal equivalent circuit model of GaAs a chip pHEMT with and without illumination has been developed based on DC and S-parameters at multiple bias points. The photoresponse of the model attributes the behaviour mainly to the photoconductive effect. The optically controlled model illustrates that the nonlinear behaviour of I_{DS} as a function of illumination is strongly dependent on the drain-to-source voltage, V_{DS}. This phenomenon does not appear in MESFETs. The model developed in this work has been successfully applied to HEMT oscillator design.

7 Acknowledgment

The authors thank Hewlett-Packard Microwave Technology Division for supply of the chip pHEMTs. They also thank A. Adams, R. Drury, H. Kazemi and X. Zhang for their kind help during the device measurement and bonding. G. Zhang acknowledge the financial support from the Sino-British Friendship Scholarship Scheme.

8 References

1 DE SALLES, A.A.A.: 'Optical control of GaAs MESFET', *IEEE Trans. Microw. Theory Tech.*, 1983, **31**, (10), pp. 813–823
2 SIMONS, R.: 'Microwave performance of an optically controlled AlGaAs/GaAs high electron mobility transistor and GaAs MESFET', *IEEE Trans. Microw. Theory Tech.*, 1987, **35**, (12), pp. 1444–1455
3 DE SALLES, A.A.A., and ROMERO, M.A.: 'AlGaAs/GaAs HEMTs under optical illumination', *IEEE Trans. Microw. Theory Tech.*, 1991, **39**, (12), pp. 2010–2017
4 BANGERT, A., ROSENZWEIG, J., HULSMANN, A., KAUFEL, G., and KOHLER, K.: 'Optical control of pseudomorphic HEMT-based MMIC oscillators', *Microw. Opt. Technol. Lett.*, 1993, **6**, (1), pp. 36–38
5 KAWASAKI, S.: 'Optical control of MMIC oscillators and model parameter analysis of illuminated FET at the Ka- and V-band'. 1995 IEEE MTT-S Int. Microw. Symp. Dig., May 1995, Orlando, Florida, USA, pp. 1287–1290
6 DAMBRINE, G., CAPPY, A., HELIODORE, F., and PLAYEZ, E.: 'A new method for determining the FET small-signal equivalent circuit', *IEEE Trans. Microw. Theory Tech.*, 1988, **36**, (7), pp. 1151–1159
7 ANGELOV, I., ZIRATH, H., and RORSMAN, N.: 'A new empirical non-linear model for HEMT and MESFET devices', *IEEE Trans. Microw. Theory Tech.*, 1993, **40**, (12), pp. 2258–226
8 RODRIGUEZ-TELLEZ, J., MEZHER, K.A., PORTILLA, O.M.C., and PATROCINIO, J.C.L.: 'A highly accurate microwave non-linear MESFET model', *Microw. J.*, 1993, **280–285**
9 GOLIO, J.M.: 'Microwave MESFETs and HEMTs' (Artech House Norway, MA, 1991)
10 TAJIMA, Y., WRONA, B., and MISHIMA, K.: 'GaAs FET large-signal model and its application to circuit designs', *IEEE Trans. Electron Devices*, 1981, **28**, (2), pp. 171–175
11 THOMASIAN, A., REZAZADEH, A.A., and HIPWOOD, L.G.: 'Observation and mechanism of kink effect in deletion-mode AlGaAs/GaAs and AlGaAs/GaInAs HEMTs', *Electron. Lett.*, 1989, **25**, (5), pp. 351–353
12 BANGERT, A., ROSENZWEIG, J., BOSCH, R., BRONNER, W., KOHLER, K., and RAYNOR, B.: 'Voltage dependence of the optical response of a pseudomorphic HFET-photodetector'. Proceedings of the 24th European Microwave Conference, Sept. 1994, France, Vol. 2, pp. 1477–1482